Intrinsic Chemistry of $[OUCH]^+$: Reactions with H_2O, $CH_3C{\equiv}N$ and O_2

Journal:	*Physical Chemistry Chemical Physics*
Manuscript ID	CP-COM-01-2021-000177.R1
Article Type:	Communication
Date Submitted by the Author:	10-Feb-2021
Complete List of Authors:	Metzler, Luke; Duquesne University Bayer School of Natural and Environmental Sciences, Farmen, Christopher T.; Duquesne University Bayer School of Natural and Environmental Sciences, Chemistry and Biochemistry Corcovilos, Theodore A.; Duquesne University, Physics van Stipdonk, Michael J.; Duquesne Univ, Chemistry and Biochemistry

COMMUNICATION

Intrinsic Chemistry of $[OUCH]^+$: Reactions with H_2O, $CH_3C{\equiv}N$ and O_2

Luke J. Metzler,[a] Christopher T. Farmen,[a] Theodore A. Corcovilos,[b] and Michael J. Van Stipdonk*[a]

Received 00th January 20xx,
Accepted 00th January 20xx

DOI: 10.1039/x0xx00000x

We report the first experimental study of the intrinsic chemistry of a U-methylidyne species, focusing on reaction of $[OUCH]^+$ with H_2O, O_2 and $CH_3C{\equiv}N$ in the gas phase. DFT was also used to determine reaction pathways, and establish the mechanism by which $[OUCH]^+$ is formed through collision-induced dissociation of $[UO_2(C{\equiv}CH)]^+$.

The high stability and inertness of the U=O bonds make activation and/or functionalization of UO_2^{2+} and UO_2^+ challenging.[1-6] However, in condensed phase reactions, it has been shown that activation and functionalization of U=O bonds can be achieved using, for example, a combination of coordination by Lewis acids and reductive silylation or by other means[7-10]. Recent gas phase experiments provide evidence that the U=O bonds of UO_2^{2+} can be activated and substituted using collision-induced dissociation (CID)[11]. For example, we have shown that $[NUO]^+$ can be created by rearrangement and fragmentation of $[UO_2(N{\equiv}C)]^+$, which was generated by homolytic C-C bond cleavage during CID of $[UO_2(N{\equiv}C\text{-}CH_3)]^{2+}$.[11b] Gibson and coworkers demonstrated that CID of $[UO_2(N_3)Cl_2]^-$ generates $[UO(NO)Cl_2]^-$ by elimination of N_2,[11d] and that $[UO_2(NCO)Cl_2]^-$ dissociates by elimination of CO_2 to create $[UONCl_2]^-$.[11e]

Recently, we showed that CID of $[UO_2(O_2C\text{-}C{\equiv}CH]^+$ can be used to prepare the organometallic species $[UO_2(C{\equiv}CH)]^+$ by decarboxylation[11f]. High-accuracy *m/z* measurements demonstrated conclusively that subsequent CID of $[UO_2(C{\equiv}CH)]^+$ caused elimination of CO to furnish $[OUCH]^+$, thus providing another example of the substitution of an oxo ligand of uranyl ion by unimolecular gas-phase reaction. Relative energies for various candidate structures and assessments of molecular orbitals and bonding[11f], based on density functional theory (DFT) calculations, suggested that the $[OUCH]^+$ ion is a uranium-methylidyne product, demonstrating one rare instance of a U≡C triple bond[12].

Our earlier report included a preliminary study of ion-molecule reactivity of $[OUCH]^+$, in which the ion was isolated for reaction with neutrals present as adventitious species in the vacuum system of the ion trap (primarily H_2O and O_2). Computed energies suggested that reaction of $[OUCH]^+$ with either H_2O or O_2 to create $[UO_2]^+$ should be spontaneous. However, the reaction was predicted to be more favorable with O_2.

Here we present studies of the intrinsic reaction of $[OUCH]^+$ with H_2O, $H_2{}^{18}O$ and $CH_3C{\equiv}N$, which were identified using multiple-stage (MS^n) tandem ion-trap mass spectrometry. Probable pathways by which respective product ions are generated were then determined with the aid of DFT calculations. DFT calculations also were used to produce a clearer picture of the pathway by which $[OUCH]^+$ may be formed from CID of $[UO_2(C{\equiv}CH)]^+$. Details of the experimental and computational approaches used are available in the supplementary information.

Our first goal was to determine the pathway by which $[UO_2]^+$ is generated by reaction with background species such as H_2O and O_2, as discussed in our earlier report[11f]. The product ion spectra generated by isolation of $[OUCH]^+$ for reaction with background H_2O and O_2 in the ion trap for periods ranging from 1 ms to 1 s are shown in Figure S1 of the supplementary information. It is important to note that in the ion-molecule reaction experiments, all ions except $[OUCH]^+$ are resonantly ejected from the LIT prior to the imposed isolation step. Any ions observed after the imposed isolation and storage period are products generated by ion-molecule reactions.

With increasing isolation and reaction time, the relative intensity of $[OUCH]^+$ at *m/z* 267 decreased, and the only product ion observed was $[UO_2]^+$ at *m/z* 270. We initially attributed formation of $[UO_2]^+$ either to reaction with H_2O, with elimination of methyl radical ($\bullet CH_3$, reaction 1), or reaction with O_2 with elimination of formyl radical ($\bullet OCH$, reaction 2).[11f]

(1) $[OUCH]^+ + H_2O \rightarrow [UO_2]^+ + \bullet CH_3$

---

[a] Department of Chemistry and Biochemistry, Duquesne University, 600 Forbes Ave. Pittsburgh, PA 15282 USA.
[b] Department of Physics, Duquesne University, 600 Forbes Ave. Pittsburgh, PA 15282 USA.

Electronic Supplementary Information (ESI) available: [details of any supplementary information available should be included here]. See DOI: 10.1039/x0xx00000x

(2) $[OUCH]^+ + O_2 \rightarrow [UO_2]^+ + \bullet OCH$

To probe whether $[UO_2]^+$ is formed by reaction with H_2O, $[OUCH]^+$ was isolated and exposed to $H_2{}^{18}O$ deliberately introduced into the LIT (Figure 1). A peak at m/z 272, which grew in intensity with increasing reaction time, is consistent with the incorporation of ^{18}O into $[UO_2]^+$ by reaction 1. The presence of the ion at m/z 270 in the spectra is attributed to reaction with $H_2{}^{16}O$ and/or molecular O_2 (both are unavoidable background species in this vacuum system[13]). Under the conditions used, no product ions other than those at m/z 270 and 272 were detected.

Energy profiles (zero-point corrected electronic energies of singlet- and triplet-state species) for reaction of $[OUCH]^+$ with H_2O are shown in Figure 2 (structures and energies are provided in the supplementary information). The calculations suggest that reaction 1 proceeds from the H_2O adduct to $[OUCH]^+$ (structure II) through proton transfer (TSII→III) to create intermediate III, which appears to be a OU-methylidene-hydroxide. A second proton transfer step (TSIII→IV) creates $[UO_2(CH_3)]^+$ (structure IV). Subsequent elimination of $\bullet CH_3$ generates $[UO_2]^+$.

The computed reaction energies suggest that reaction 1 should be spontaneous, consistent with the appearance of the peak at m/z 272 created by reaction of $[OUCH]^+$ with $H_2{}^{18}O$. The DFT results also suggest that the reaction occurs primarily on the singlet-state energy profile, though some contribution of triplet state species cannot be ruled out, particularly when considering the transition state for the second H transfer step (TSIII→IV) to create the $[UO_2(CH_3)]^+$ intermediate.

The ion trap used here is not currently adapted to allow the introduction of gaseous reagents, which prevented an investigation of the reaction with 18-O labeled molecular oxygen. However, our calculations (Figure 2) suggest that reaction with O_2 should be significantly more favorable that reaction with H_2O. In fact, we were not able to locate a minimum for the encounter complex, $[OUCH\text{-}(O_2)]^+$. Instead, addition of O_2 to $[OUCH]^+$ in either end-on or side-on fashion lead spontaneously to formation of the UO_2 complex with OCH (structure V) during optimization. Subsequent elimination of formyl radical leads to $[UO_2]^+$ at m/z 270. Because reaction with H_2O or O_2 creates $[UO_2]^+$ (a U(V) species) from $[OUCH]^+$ (formally U(VI)) it is likely that inclusion of spin-orbit effects would decrease the overall reaction energy[14].

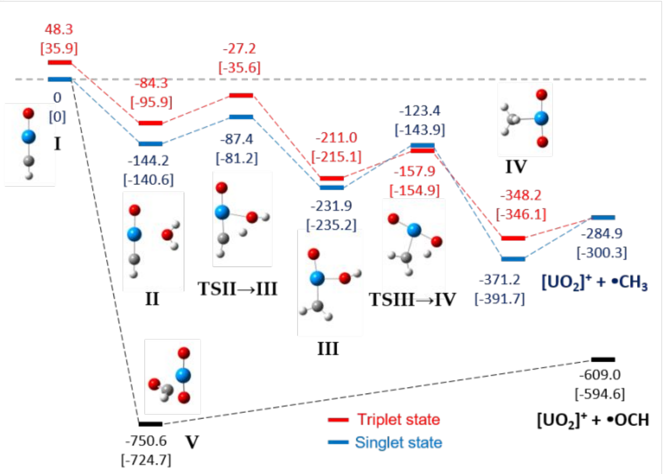

Figure 1. Computed energy diagram for reaction of $[OUCH)]+$ with H_2O and O_2 using zero-point corrected electronic energies in kJ/mol at the M06L and PBE0 (in brackets) level of theory. The energies shown in black represent the formation of $[UO_2]^+$ by reaction with O_2, with singlet state for intermediate with formyl ligand, and doublet state for the U(V) dioxocation.

Reaction with acetonitrile ($CH_3C\equiv N$) was also investigated. Our hypothesis was that substitution of nitride for methylidyne, with associated C-C coupling to create (neutral) propyne (reaction 3), would be observed. The product ion spectra generated by isolation of $[OUCH]^+$ for reaction with $CH_3C\equiv N$ introduced into the ion trap for periods ranging from 1 ms to 1 s are shown in Figure 3. With increasing reaction time, prominent product ion peaks at m/z 268 and 270 were observed. The former is consistent with formation of $[NUO]^+$ and propyne as the complementary neutral species by reaction 3. The latter is assumed to be $[UO_2{}^+]$ and attributed to reaction with background H_2O and/or O_2. Under the conditions used, no product ions other than those at m/z 268 and 270 were detected.

(3) $[OUCH]^+ + CH_3C\equiv N \rightarrow [NUO]^+ + HC\equiv CCH_3$

Energy profiles for reaction of $[OUCH]^+$ with $CH_3C\equiv N$ are shown in Figure 4 (structures and energies are provided in the supplementary information). The calculations suggest that reaction with $CH_3C\equiv N$ proceeds along a pathway that involves initial folding of the encounter complex (structure VI) through transition state TSVI→VII to create an insertion intermediate VII that includes a new C-C bond. Subsequent C-N bond cleavage through transition state TSVII→VIII creates an ion-molecule complex between $[NUO]^+$ and $CH_3C\equiv CH$ (structure VIII). Elimination of the propyne ligand leaves the $[NUO]^+$ product (structure IX). The calculations indicate that formation of $[NUO]^+$ should be spontaneous, which result is consistent with our experimental observation. The computed energetics also

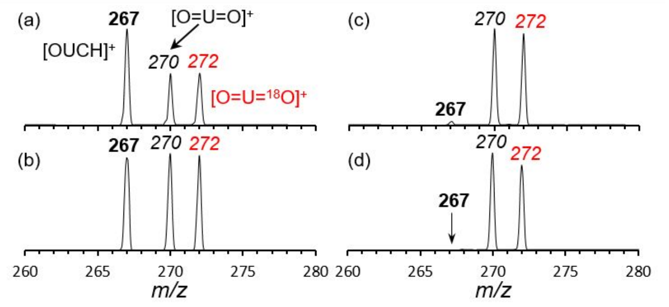

Figure 2. Product ion spectra generated by reaction of $[OUCH]^+$ with $H_2{}^{18}O$ (~ $1x10^{-6}$ torr). Isolation/reaction periods shown are: (a) 1 ms, (b) 10 ms, (c) 100 ms and (d) 1 s.

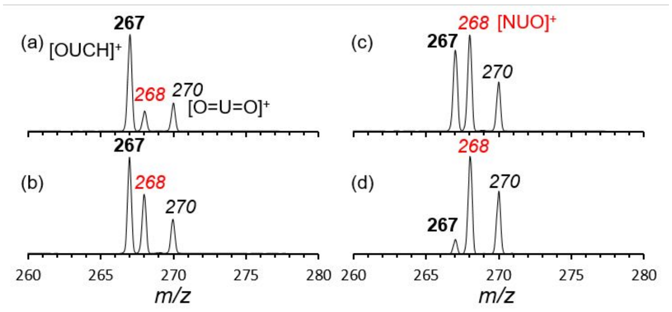

Figure 3. Product ion spectra generated by reaction of $[OUCH]^+$ with $CH_3C\equiv N$ (~ $1x10^{-6}$ torr). Isolation/reaction periods shown are: (a) 1 ms, (b) 10 ms, (c) 100 ms and (d) 1 s.

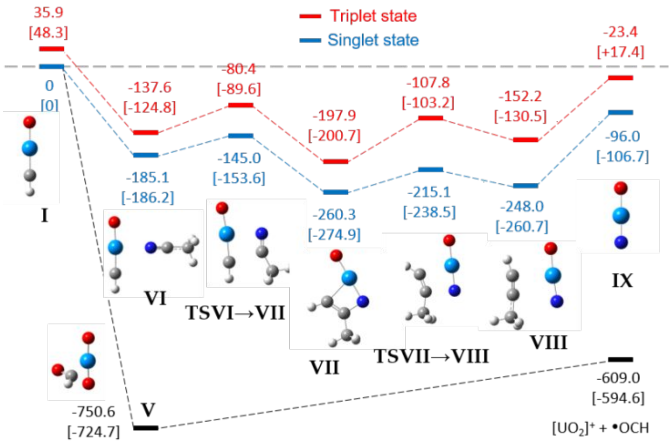

Figure 4. Computed energy diagram for reaction of $[OUCH)]^+$ with $CH_3C{\equiv}N$ using zero-point corrected electronic energies in kJ/mol at the M06L and PBE0 (in brackets) level of theory.

suggest that there is no contribution of triplet state species, and because there is no net change in formal oxidation state of U in the reaction with $CH_3C{\equiv}N$, spin-orbit effects are assumed to be negligible.

The use of CID to prepare the U-methylidyne species in the gas phase was discussed in our earlier report, and readers are directed to ref. 11f for details about the use of MS^n CID and accurate mass measurement to establish the creation of $[OUCH]^+$. One caveat in the earlier study was that our argument neglected any potential reaction barriers associated with rearrangement(s) necessary to generate $[OUCH]^+$ by loss of CO. Therefore, our final goal was to identify the pathway by which $[OUCH]^+$ is formed by CID of $[UO_2(C{\equiv}CH)]^+$, and determine if the pathway is competitive against elimination of $C{\equiv}CH$ radical to create $[UO_2]^+$ as the terminal MS^n product ion (the dominant dissociation channel observed in a prior investigation[13b] that involved CID of $[UO_2(R)]^+$, $R{=}CH_3$, CH_2CH_3, $CH{=}CH_2$ and C_6H_5).

Relevant structures and energies are provided in the supplementary information. The reaction energy profiles for the dissociation of $[UO_2(C{\equiv}CH)]^+$ are provided in Figure 5. Our calculations suggest that formation of $[OUCH]^+$ likely proceeds through a multi-step mechanism that involves a double crossing between the singlet and triplet energy surfaces of the system. The $[UO_2(C{\equiv}CH)]^+$ (structure X) precursor is lowest in energy on the singlet surface. The first crossing occurs after the first transition state (TSX→XI) to form an $[OU(C\text{-}CH\text{-}O)]^+$ insertion intermediate (structure XI). Transfer of H (through TSXI→XII) creates a second insertion intermediate $[OU(CH\text{-}C\text{-}O)]^+$ (structure XII). No alternative pathway to intermediate XII was identified. Surprisingly, at the M06L level of theory, the computed energy of structure XII in the triplet state is only 14.2 kJ/mol higher in energy than $[UO_2(C{\equiv}CH)]^+$ (11.1 kJ/mol higher at the PBE0 level of theory), a result similar to the reported mechanism for generation of $[NUO]^+$ from $[UO_2(C{\equiv}N)]^+$.[26] The reaction then crosses a second time and proceeds toward the formation of the reaction products, $[OUCH]^+$ + CO, on the singlet-state surface through a third transition state (TSXII→XIII) that involves the breaking of the OC-CH bond.

At the level of theory used here, with the double crossing of the surfaces, production of $[OUCH]^+$ (structure I) by rearrangement of $[UO_2(C{\equiv}CH)]^+$ is favored over ejection $C{\equiv}CH$ radical to make $[UO_2]^+$ (structure XIV). No pathway was identified that leads to formation of alternative ions such as $[CUOH]^+$ or $[HUCO]^+$.

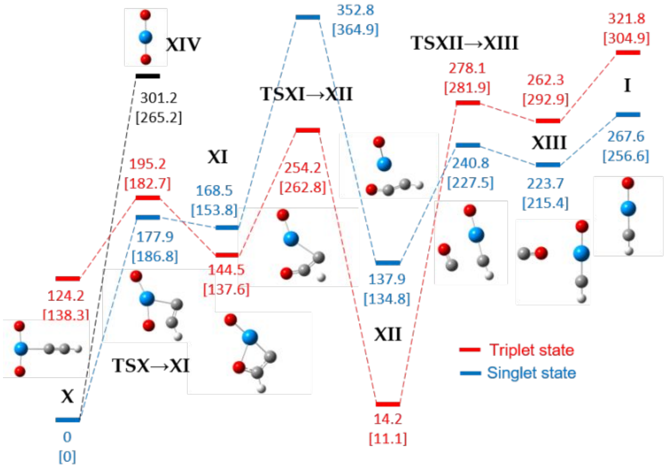

Figure 5. Computed reaction energy diagram for dissociation of $[UO_2(C{\equiv}CH)]^+$. The energies shown in black represent the formation of $[UO_2]^+$ by elimination of $C{\equiv}CH$ radical.

The importance of "two-state reactivity" in gas-phase organometallic chemistry[15] and the chemistry of electronic excited states[16] has been summarized nicely elsewhere. We note that our DFT study of the pathway by which $[OUCH]^+$ is formed, including the crossings of the singlet and triplet-state energy profiles, is very similar to the mechanism proposed in our earlier study[26] of the formation of $[NUO]^+$ from $[UO_2(C{\equiv}N)]^+$, which provides additional confidence that the formation of $[OUCH]^+$ occurs as depicted in Figure 5.

While spin-orbit effects were not included in our computed reaction energetics, previous computational studies have shown that spin–orbit corrections can lower energies of reactions that involve $U^{VI}O_2$ and $U^{V}O_2$ by ca. 30 kJ/mol because of stabilization of open-shell U(V) species[14]. We note that at the M06L level of theory, correction of the reaction energies by a similar magnitude would still leave the rearrangement mechanism competitive, if not lower in energy, than the radical-ejection pathway. Based on reports from advanced theoretical calculations[17] and condensed-phase experiments[18] we expect that spin-orbit effects for the U 5*f* orbitals could enhance the coupling between the singlet and triplet potential energy surfaces[19].

To summarize, we used ion-trap mass spectrometry and DFT to investigate of the reaction of $[OUCH]^+$ with H_2O and $CH_3C{\equiv}N$. To the best of our knowledge, this represents the first experimental investigation of the intrinsic reactivity of a gas-phase uranium-carbyne species. Using ^{18}O-labeled water we discovered that $[OUCH]^+$ reacts spontaneously to create $[UO_2]^+$, likely through a series of H-transfer steps to create an $[UO_2(CH_3)]^+$ intermediate and subsequent elimination of methyl radical. The $[OUCH]^+$ ion reacts spontaneously with $CH_3C{\equiv}N$ to create $[NUO]^+$, and calculations suggest a mechanism that involves substitution of nitride for methylidyne, and C-C bond formation to create propyne as the complementary (neutral) product. Though not discussed here, preliminary investigations also showed that $[NUO]^+$ is also created by reaction with propionitrile, presumably with concomitant generation of butyne as the neutral product. Though we could not perform experimental measurements with isotopically labeled gas, DFT calculations suggest that reaction of $[OUCH]^+$ with O_2 will be favored significantly over reaction with either H_2O or $CH_3C{\equiv}N$. The reaction appears to create $[UO_2]^+$ by elimination of a formyl radical.

Our calculations also suggest that $[OUCH]^+$ is created in a multi-step process that involves C-O bond formation, H transfer, and subsequent C-C bond cleavage to create a U-carbyne (methylidyne) species. Important to the mechanism is two crossings of the singlet and triplet energy surfaces that make the rearrangement competitive with direct elimination of $C{\equiv}CH$ radical from $[UO_2(C{\equiv}CH)]^+$ during CID, and no pathways to alternative structures such as $[CUOH]^+$ or $[HUCO]^+$ were identified. The calculations provide further supporting evidence for the substitution of an oxo ligand of uranyl ion by unimolecular gas-phase reaction.

Author Contributions

LJM: Investigation, Methodology and Validation. CTF: Investigation and Methodology. TAC: Conceptualization, Methodology, Writing – review & editing. MJV: Conceptualization, Methodology, Writing – original draft, Project administration.

Notes and references

1. S. Fortier, T. W. Hayton, Oxo ligand functionalization in the uranyl ion (UO_2^{2+}). *Coord. Chem. Rev*. 2010, **254**, 197 – 214.

2. R. J. Baker, New reactivity of the uranyl(VI) ion. *Chem. Eur. J*. 2012, **18**, 16258 – 16271.

3. M. B. Jones, A. J. Gaunt, Recent developments in synthesis and structural chemistry of non-aqueous actinide complexes. *Chem. Rev*. 2013, **113**, 1137 – 1198.

4. B. E. Cowie, J. M. Purkis, J. Austin, J. B. Love, P. L. Arnold, Thermal and photochemical reduction and functionalization chemistry of the uranyl dication, $[U^{VI}O_2]^{2+}$. *Chem. Rev*. 2019, **119**, 10595-10637.

5. P. L. Arnold, J. B. Love, D. Patel, Pentavalent uranyl complexes. *Coord. Chem. Rev*. 2009, 253, 1973-1978.

6. M. J. Sarsfield, M. Helliwell, Extending the chemistry of the uranyl ion: Lewis acid coordination to a U=O oxygen. *J. Am. Chem. Soc*. 2014, **126**, 1036 - 1037.

7. (a) P. Arnold, D. Patel, A. J. Blanke, C. Wilson, J. B. Love, Selective oxo functionalization of the uranyl ion with 3d metal cations. *J. Am. Chem. Soc*. 2006, **128**, 9610 – 9611.; (b) P. L. Arnold, D. Patel, C. Wilson, J. B. Love, Reduction and selective oxo group silylation of the uranyl dication. *Nature*, 2008, **451**, 315 – 317.; (c) G. M. Jones, P. L. Arnold, J. B. Love, Controlled deprotection and reorganization of uranyl oxo groups in a binuclear macrocyclic environment. *Angew. Chem. Int. Ed*. 2012, **51**, 12584 – 12587.; (d) N. L. Bell, P. L. Arnold, J. B. Love, Controlling uranyl oxo group interactions to group 14 elements using polypyrrolic Schiff-base macrocyclic ligands, *Dalton Trans.* **2016**, *45*, 15902 – 15909.; (e) P. L. Arnold, A.-F. Pecharman, E. Hollis, A. Yahia, L. Maron, A. Parsons, J. B. Love, Uranyl oxo activation and functionalization by metal cation coordination. *Nat. Chem*. 2010, **12**, 1056 – 1061.; (f) P. L. Arnold, E. Hollis, G. S. Nichol, J. B. Love, J.-C. Griveau, R. Caciuffo, N. Magnani, L. Maron, L. Castro, A. Yahia, S. O. Odoh, G. Schreckenback, Oxo-functionalization and reduction of the uranyl ion through lanthanide-element bond hemolysis: synthetic, structural, and bonding analysis of a series of singly reduced uranyl-rare earth 5f1-4fn complexes. *J. Am. Chem. Soc*. 2013, **135**, 3841 – 3854.; (g) P. L. Arnold, A.-F. Pecharman, R. M. Lord, G. M.; Jones, E. Hollis, G. S. Nichol, L. Maron, J. Fang, T. Davin, J. B. Love, Control of oxo-group functionalization and reduction of the uranyl ion. *Inorg. Chem*. 2015, **54**, 3702 – 2710.; (h) M. Zegke, G. S. Nichol, P. L. Arnold, J. B. Love, Catalytic one-electron reduction of uranyl(VI) to Group 1 uranyl(v) complexes via Al(III) coordination. *Chem. Commun*., 2015, **51**, 5876-5879. (i) N. L. Bell, B. Shaw, P. L. Arnold, J. B. Love, Uranyl to uranium(IV) conversion through manipulation of axial and equatorial ligands. *J. Am. Chem. Soc*. 2018, **140**, 3378-3384.

8. (a) D. D. Schnaars, G. Wu, T. W. Hayton, Reduction of pentavalent uranyl to U(IV) facilitated by oxo functionalization. *J. Am. Chem. Soc*. 2009, **131**, 17532 – 17533.; (b) T. W. Hayton, G. Wu, Exploring the effects of reduction or Lewis acid coordination on the U=O bond of the uranyl moiety. *Inorg. Chem*. 2009, **48**, 3065 – 3072.; (c) D. D. Schnaars, G. Wu, T. W. Hayton, Silylation of the uranyl ion using $B(C_6F_5)_3$-activated Et_3SiH. *Inorg. Chem*. 2011, **50**, 9642 – 9649.; (d) E. A. Pedrick, G. Wu. N. Kaltsoyannis, T. W. Hayton, Reductive silylation of a uranyl dibenzoylmethanate complex: an example of controlled uranyl oxo ligand cleavage. *Chem. Sci*. 2014, **5**, 3204 – 3213.; (e) L. A. Seaman, E. A. Pedrick, G. Wu, T. W. Hayton, Promoting oxo functionalization in the uranyl ion by ligation to ketimides. *J. Organomet. Chem*. 2018, **857**, 34 – 37.; (f) E. A. Pedrick, G. Wu, T. W. Hayton, Oxo ligand substitution in a cationic uranyl complex: synergistic interaction of an electrophile and a reductant. *Inorg. Chem*. 2015, **54**, 7038 – 7044.

9. (a) J. J. Kiernicki, D. P. Cladis, P. E. Fanwick, M. Zeller, S. C. Bart, Synthesis, characterization, and stoichiometric U-O bond scission in uranyl species supported by pyridine(diamine) ligand radicals. *J. Am. Chem. Soc*. 2015, **137**, 11115 – 11125.; (b) E. J. Coughlin, Y. Qiao, E. Lapsheva, M. Zeller, E. J. Schelter, S. C. Bart, Uranyl functionalization mediated by redox-active ligands: generation of O-C- bonds via acylation. *J. Am. Chem. Soc*. 2019, **141**, 1016–1026.

10. A. J. Lewis, P. J. Carroll, E. J. Shelter, Stable uranium(VI) methyl and acetylide complexes and the elucidation of an inverse trans influence ligand series. *J. Am. Chem. Soc*. 2013, **135**, 13185–13192.

11. (a) R. A. Abergel, W. A. de Jong, G. J-P. Deblonde, P. D. Dau, I. Captain, T. M. Eaton, J. Jian, M. J. van Stipdonk, J. Martens, G. Berden, J. Oomens, J. Gibson, Cleaving off uranyl oxygens through chelation: A mechanistic study in the gas phase. *Inorg. Chem*. 2017, **56**, 12930 – 12937. (b) M. J. Van Stipdonk, M. del Carmen Michelini, A. Plaviak, D. Martin, J. K. Gibson, Formation of bare UO_2^{2+} and NUO^+ by fragmentation of gas-phase uranyl-acetonitrile complexes. *J. Phys. Chem. A*. 2014, **118**, 7838 – 7846.; (c) S.-X. Hu, J. Jian, J. Li, J. K. Gibson, Destruction of the uranyl moiety in a U(V) “cation-cation” interaction. *Inorg. Chem*. 2019, **58**, 10148 – 10159.; (d) Y. Gong, V. Vallet, M. Michelini, D. Rios, J. K. Gibson, Activation of gas-phase uranyl: from and oxo to a nitrido complex. *J. Phys. Chem. A*. 2014, **118**, 325 – 330.; (e) Y. Gong, W. A.; de Jong, J. K. Gibson, Gas phase uranyl activation: formation of a uranium nitrosyl complex from uranyl azide. *J. Am. Chem. Soc*. 2015, **137**, 5911 – 5915. (f) M. J. van Stipdonk, I. J. Tatosian, A. C. Iacovino, A. R. Bubas, L. Metzler, M. C. Sherman, A. Somogyi, Gas-phase deconstruction of UO_2^{2+}: Mass spectrometry evidence for generation of $[OU^{VI}CH]^+$ by collision-induced dissociation of $[U^{VI}O_2(C{\equiv}CH)]^+$. *J. Am. Soc. Mass Spectrom.* 2019, **30**, 796 – 805.;

12. J. T. Lyon, H.-S. Hu, L. Andrews, J. Li, Formation of unprecedented actinide≡carbon triple bonds in uranium methylidine molecules. *Proc. Nat. Acad. Sci*. 2007, **104**, 18919 – 18924.

13. (a) C. M. Leavitt, V. S. Bryantsev, W. A. de Jong, M. S. Diallo, W. A. Goddard III, G. S. Groenewold, M. J. Van Stipdonk, Addition of H_2O and O_2 to acetone and dimethylsulfoxide ligated uranyl(V) dioxocations. *J. Phys. Chem. A*. 2009, **113**, 2350 – 2358.; (b) M. Van Stipdonk, E. Perez, C. Hanley, I. Tatosian, A. Bubas, S. Kline, Formation and hydrolysis of gas-phase $[U^{VI}O_{2(}R)]^+$ [R=CH_3, CH_2CH_3, CH=CH_2 and C_6H_5]. *J. Mass Spectrom. 2019,* **54**, 780 – 789.

14. (a) V. Vallet, B. Schimmelpfenning, L. Maron, C. Teichteil, T. Leininger, O. Gropen, I. Grenthe, U. Wahlgren, Reduction of uranyl by hydrogen: an Ab Initio Study. *Chem. Phys*. 1999, **244**, 185−193.; (b) V. Vallet, L. Maron, B; Schimmelpfenning, T. Leininger, C; Teichteil, O. Gropen, I. Grenthe, U. Wahlgren, Reduction Behavior of the early actinyl ions in aqueous solution. *J. Phys. Chem. A* 1999, **103**, 9285−9289.; (c) P. J. Hay, R. L. Martin, G. Schreckenbach, Theoretical studies of the properties and solution chemistry of AnO_2^{2+} and AnO_2^+ aquo complexes for An = U, Np, and Pu. *J. Phys. Chem. A* 2000, **104**, 6259−6270.; (d) G. A. Shamov, G. Schreckenbach, Density functional studies of actinyl aquo complexes studied using small-core effective core potentials and a scalar four-component relativistic method. *J. Phys. Chem. A* 2005, **109**, 10961−10974.; (e) S. Tsushima, U. Wahlgren, I. Grenthe, Quantum chemical calculations of reduction potentials of AnO_2^{2+}/AnO_2^+ (An = U, Np,Pu, Am) and Fe^{3+}/Fe^{2+} Couples. *J. Phys. Chem. A* 2006, **110**, 9175−9182.

15. D. Schröder, S. Shaik, H. Schwarz, Two-state reactivity as a new concept in organometallic chemistry. *Acc. Chem. Res*. 2000, **33**, 139-145.

16. P. B. Armentrout, Chemistry of excited electronic states. *Science*, 1991, **251**, 175-179.

17. (a) N. Kaltsoyannis, Transuranic computational chemistry. *Chem. Eur. J*. 2018, **24**, 2815–2825.; (b) J. T. Pegg, A. E. Shields, M. T. Storr, D. O. Scanlon, N. H. de Leeuw, Noncollinear relativistic DFT + U calculations of actinide dioxide surfaces. *J. Phys. Chem. C*, 2019, **123**, 356–366.; (c) U. D. Wdowik, P. Piekarz, D. Legut, G. Jagło, Effect of spin-orbit and on-site coulomb interactions on the electronic structure and lattice dynamics of uranium monocarbide. *Phys. Rev. B* 2016, **94**, 054303.

18. T. Vitova, I. Pidchenko, D. Fellhauer, P. S. Bagus, Y. Joly, T. Pruessmann, S. Bahl, E. Gonzalez-Robles, J. Rothe, M. Altmaier, M. A. Denecke, H Geckeis, The role of the 5f valence orbitals of early actinides in chemical bonding. *Nat Commun* 2017, **8**, 16053; (b) I. D. Prodan, G. E; Scuseria, R. L. Martin, Covalency in the actinide dioxides: systematic study of the electronic properties using screened hybrid density functional theory. *Phys. Rev. B* 2007, **76**, 033101.

19. C. M. Marian, Spin–orbit coupling and intersystem crossing in molecules. *WIRES Comput. Mol. Sci*. 2012, **2**, 187–203.